New quantum assignments and analysis of high-resolution H212CO spectra in the range 3700–4450 cm-1

A.V. Nikitin, A.A. Rodina, A.E. Protasevich, L. Manceron, Michael M. Rey, V.G. Tyuterev

New quantum assignments and analysis of high-resolution $H_2{}^{12}CO$ spectra in the range 3700-4450 cm^{-1}

A.V. Nikitin[1], A.A. Rodina[1], A.E. Protasevich[1], L. Manceron[2,3], M. Rey[4], V. G. Tyuterev[1]

[1.,] *V.E. Zuev Institute of Atmospheric Optics, Russian Academy of Sciences, 1 Akademichesky Avenue, 634055 Tomsk, Russian Federation*

[2.,] *AILES Beamline, Synchrotron SOLEIL, L'Orme des Merisiers, St-Aubin BP48, F-91192 Gif-sur-Yvette Cedex, France*

[3.,] *LISA, CNRS, Université Paris Cité and Univ Paris Est Creteil, F-75013 Paris, France*

[4.,] *Groupe de Spectrometrie Moleculaire et Atmospherique, UMR CNRS 6089, Universite de Reims, U.F.R. Sciences, B.P. 1039, 51687 Reims Cedex 2, France*

Number of Pages: 21
Number of Figures: 9
Number of Tables: 4
Number of supplemental files: 2

Keywords: high resolutions spectra; dipole moment; formaldehyde; vibration-rotation states; infrared absorption; effective Hamiltonian

Correspondence should be addressed to:
Andrei V. Nikitin,
*Laboratory of Theoretical Spectroscopy, V.E. Zuev Institute of Atmospheric Optics, SB RAS, 1 Akademichesky Avenue, 634055 Tomsk, Russia
E-mail: avn@iao.ru
Tel. +73822 - 491111, ext. 1260

Abstract:

Four spectra of formaldehyde in natural isotopic abundance in the 3700-5200 cm^{-1} region were recorded at low temperature 160-166 K at Synchrotron SOLEIL for various pressures. Line positions and intensities were retrieved by non-linear least-squares curve-fitting procedures in the range 3700-4450 cm^{-1} and analyzed using ab initio based effective Hamiltonian and line intensities computed using new ab initio dipole moment surface. A new measured line list contains positions and intensities for 6177 features. Refined parameters of effective Hamiltonian were fitted to all assigned line positions with the RMS deviations of 0.001 cm^{-1}. Updated line lists include intensity values based on ab initio variational calculations which were subsequently empirically optimized. Comparison of our theoretical simulation with previously available data as well as with high-resolution and low-resolution experimental spectra are reported.

Introduction

Accurate data on the absorption of formaldehyde can be used for the retrieval of this molecule in various environments. This molecule is relatively abundant in the interstellar medium [1], was found in comets [2] and in proto-planetary discs around some stars [3]. It was classified as genotoxic cancerogenic species [4] and is considered as an environmental pollutant in the atmosphere [5], [6], [7], [8]. Improved line-by-line analyses are required for the interpretation of spectra recorded by the ground-based and satellite observatories [9], [10].

Such analyses can be efficiently assisted by theoretical predictions of spectra using *ab initio* potential energy surfaces (PES) and of dipole moment surfaces (DMS). This was the case of some recent variational calculations for three-atomic [11], [12], [13], [14], [15], four-atomic [16], [17], [18] and five-atom molecules [19], [20], [21], [22], [23] where *ab initio* based approaches helped better modelling and assignments of high-resolution spectra. Many *ab initio* PESs have been subsequently refined by a fit to experimental data to achieve better accuracy in line positions. Theoretical line lists for ammonia [16], [24] and phosphine [25], [17], [18] are successful examples of this trend for four-atomic species. New PESs and DMSs have been recently reported for five-atomic [26], [27], [28], [29] six-atomic molecules [30], [31], [32], [33] and seven-atomic [34] [35] molecules.

The formaldehyde molecule was often considered as a benchmark molecule for theoretical models and high-level quantum-chemical calculations where different methods were conducted in various coordinate systems. Burleigh et al. [36] have empirically refined the CCST(T)/cc-pVTZ *ab initio* quartic force field of Martin et al. [37] using observed transition frequencies available at that time. A review of earlier works refs [36], [37], [38], [39], [40] that reported calculations of the formaldehyde PES and energy levels can be found refs. [41], [42]. First calculations of ab initio dipole moments of the formaldehyde molecule have been reported by Poulin et al [43] and by Carter et al [44]. The latter work provided rovibrational energies and dipole transition intensities for polyatomic molecules using MULTIMODE method. Yachmenev et al. [42] have calculated an *ab initio* PES in a wide range of geometries at the CCSD(T)/aug-cc-pVQZ level of the theory. Al-Refaie et al. [45] have worked out an extensive rotation-vibration line list of $H_2{}^{12}C^{16}O$ up temperatures of 1500 K, as part of the ExoMol project [46]. They empirically refitted the PES of Yachmenev et al. [15] because the previous work did not provide correct intensity predictions, and re-calculated the DMS also at the CCSD(T)/aug-cc-pVQZ level of theory in the frozen-core approximation using CFOUR code [47]. Morgan et al. [41] have published a very thorough study of the quartic force fields of formaldehyde near equilibrium using CCSDT(Q) ansatz with the CBS extrapolation and have obtained an excellent agreement vs experiment for the equilibrium structure and for low vibration levels. In our previous work [48], we reported *ab initio* PES that provided the RMS (obs.-calc.) errors of 0.25 cm^{-1} for fifteen vibrational band centers. The average error dropped to 0.08 cm^{-1} for an empirically optimized PES with six adjusted parameters, which was used to compute theoretical band origins up to 7000 cm-1.

Experimental formaldehyde spectra have been studied in many groups including MW and IR spectral ranges. The early work was reviewed by Clouthier and Ramsay (1983) [49] . Since then, the analyses of high-resolution spectra recorded with various experimental techniques in mid-IR were published in [50] [51] [52] [53] [54] [55] [56] [57] [58], [59]. Large number of experimental transitions were measured by Flaud et al. [60], Perrin et al. [61] [62] and KwabiaTchana et al. [63]. Rotationally-resolved absorption spectra from 1.4 to 1.6 μm were recorded by Ruth et al. [64] and Fjodorov et al. [65]. Vibrational band origins from low resolution dispersed laser-induced fluorescence data were reported by Bouwens et al [66]. Al-Derzi et al. [67], have collected experimental positions of assigned lines to determine empirical values of vibration-rotation levels in the electronic ground state using Marvel code [68]. They have used these empirical levels to update line positions of the ExoMol line list available at [69]. Recently German at al [70] have used optical frequency comb Fourier transform spectroscopy to record low-

pressure, room temperature spectra of $H_2{}^{12}C^{16}O$ in the range of 1250 to 1390 cm- 1 with the 0.4 MHz median uncertainty for the measured lines. These data were used to update MARVEL empirical levels, however the resulting line list did not have yet high-resolution accuracy in the range considered in our work.

Despite the importance of formaldehyde for various applications and significant progress in the measurements and analyses, this molecule remains relatively less studied compared to main atmospheric species in terms of the number of experimentally assigned bands. One of the possible reasons for this is the unavailability of the cold spectra caused by the high temperature of congelation and a complex technique for creating the formaldehyde gas. While for methane over 200 assigned vibrational energy levels have been measured with high accuracy ([71]**,** [72], [73], [74], [75], [76], [77], [78], [79] and references therein) , in case of formaldehyde, the recent lists [67], [70] extracted from high resolution rotationally resolved spectra contain the rovibrational levels of only 25 vibrational states. Currently, the HITRAN [80] and GEISA [81] databases, which are the major source of publicly available spectroscopic data, include the transitions of H_2CO in the range below 3100 cm^{-1}.

The aim of the present work is two-fold: theoretical levels of formaldehyde computed from *ab initio* PES [48] were used to extend analyses of high-resolution spectra in the 3700-4450 cm^{-1} region, whereas new *ab initio* DMS was used for intensity calculations.

The scheme of vibrational polyads of H_2CO and the band origin corresponding to our spectra range is given in Fig 1. The Polyad 3 band system contains 28 upper state vibrational levels. In this work we have analyzed 18 bands in the considered spectral range.

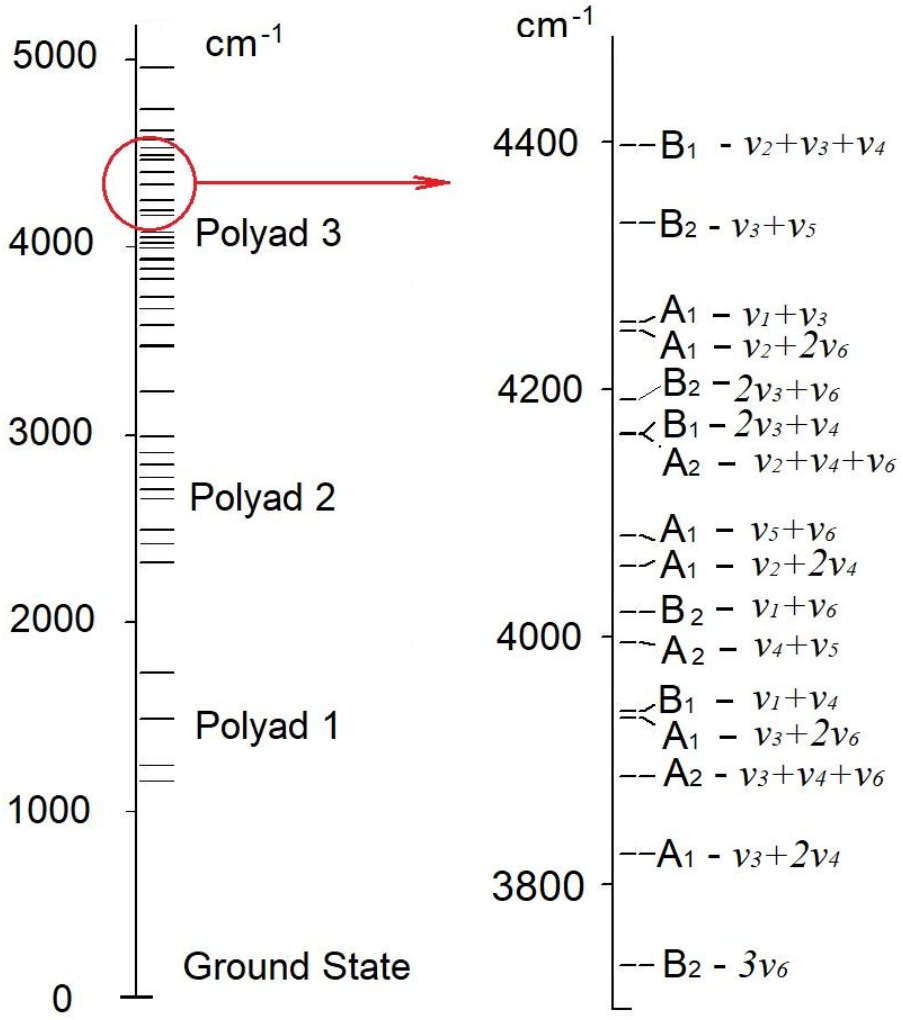

Fig. 1. *Vibrational levels of the H_2CO polyads (left side), and the vibrational band origins (right side) corresponding to rovibrational bands analyzed in this work. The right hand side panel displays the principal vibration quantum numbers (notation $v_1v_2v_3v_4v_5v_6$), and symmetry types of vibration levels within the Polyad 3. The symmetry types correspond to irreducible representations of the C_{2v} point group.*

This paper is structured as follows. The experimental conditions are described in Section 2. Ab initio DMS calculations are outlined in Section 3 whereas the transformation of the full nuclear motion Hamiltonian to the effective one for the Polyad 3 is considered in Section 4. Section 5 is devoted to the modeling and assignments of experimental spectra. New line list in the 3700-4450 cm^{-1} range and comparisons with other sources of data are discussed in the conclusion Section 6.

2. Experiment

Four absorption spectra of formaldehyde were recorded with a Bruker IFS 125 HR high-resolution Fourier transform spectrometer (FTS) using the cryogenic long path optical cell located on the AILES beamline of the SOLEIL synchrotron [63]. The instrument was fitted with a tungsten source, an entrance aperture set to 1.0 mm, a Si/CaF_2 beam splitter, a 1.3 mm aperture and 418 mm focal length collimator, and an InSb detector cooled down to 77 K. Formaldehyde was generated by slow thermal decomposition of paraformaldehyde (Sigma Aldrich, 95% purity) in a high vacuum glass line. The resulting product was then distilled twice at low temperature (-90°C) and stored at low temperature in a glass bulb before being sublimed directly in the low temperature cell. It contained a trace amount of CO_2 but did not present any evidence of decomposition or repolymerization at the low cell temperature about 160K). The pressures were measured with a Pfeiffer capacitance manometer of 10 mbar full-scale range, temperature stabilized at 45°C and characterized by an accuracy of reading of 0.1%.

An optical path length of 93 meters was adopted for all spectra. The spectra were successively recorded near 160K. About four days were needed to achieve this temperature with a 2 K temperature gradient. The varying parameters for all spectra are given in **Table 1**. All the interferograms were recorded with a maximum optical path difference (MOPD) of 150 cm, corresponding to a spectral resolution of 0.006 cm^{-1} (0.9/MOPD, according to the Bruker definition of the spectral resolution) and were transformed without apodization function (Boxcar option) with a zero-filling factor of 8. The number of interferograms averaged to yield the single beam spectra is provided in **Table 1**. The transmittance spectra were obtained after division by a zero-absorption spectrum recorded with the cell evacuated and a 0.06 cm^{-1} spectral resolution. The recordings cover the range 2500 to 7000 cm^{-1} but are mostly dedicated to the 3900-6500 cm^{-1} range where the absorption amplitude allows for quantitative measurements. At the low pressures and temperatures used here, the Doppler width is always larger than the resolution and even than the width of the sync function (0.004 cm^{-1}).

Accurate calibration of the frequency axis was achieved using CO_2 impurity lines and a high resolution N_2O spectrum and line positions provided in the HITRAN database [80] (with the uncertainties in the 10^{-3}-10^{-4} cm^{-1} range). After calibration, an RMS deviation of the position differences of about 3×10^{-4} cm^{-1} was achieved.

Table 1. Experimental conditions for series of H_2CO spectra in the range of Polyad 3.

Spectrum ID	Scan number	Pressure (Torr)	Temperature (K)
TrCH2O_2hPa	240	0.015	166
TrCH2O_7Pa	720	0.053	160
TrCH2O_22Pa	1620	0.165	165
TrCH2O_45Pa	360	0.315	163

3. Ab initio dipole moment in normal coordinates

To find the dipole moment surface (DMS), the X, Y, Z components of the dipole moment were calculated using the coupled clusters CCSD(T) method with the aug-pVTZ atomic basis set (in abbreviated AVTZ notations in what follows) on a large grid of 15000 nuclear geometries. The finite difference method for all three components was used for calculation. Additionally, on a smaller grid of 2120 geometries at the bottom of the potential well, the dipole moment was calculated using larger ACVQZ basis. We computed the analytical DMS differences $diff_2(S_i) = ACVQZ - AVTZ$ involving two basis sets where the notation S_i (i=1,…6) stands for symmetrized internal vibrational coordinates. These differences can be provide the energy corrections due to the account of augmented orbitals and of core-valence correlation at X=4 cardinal number. They were modeled analytically using the fourth-order expansions in S_i . Since the full-grid direct MOLPRO calculations with the AVTZ basis set were already available the dipole moment $ACVQZ = diff_2(S_i) + AVTZ$ was then evaluated for all remaining 15000-2120 geometries. The total DMS computed at the CCSD(T)/ACVQZ level of ab initio theory was analytically modelled in the form of a 5-th order expansion in symmetrized S_i coordinates, with the RMS fit deviation of 0.00005 a.u. The scatter of the fit deviations between our analytical DMS representation and ab initio points is given in **Fig. 2** as function of the energy.

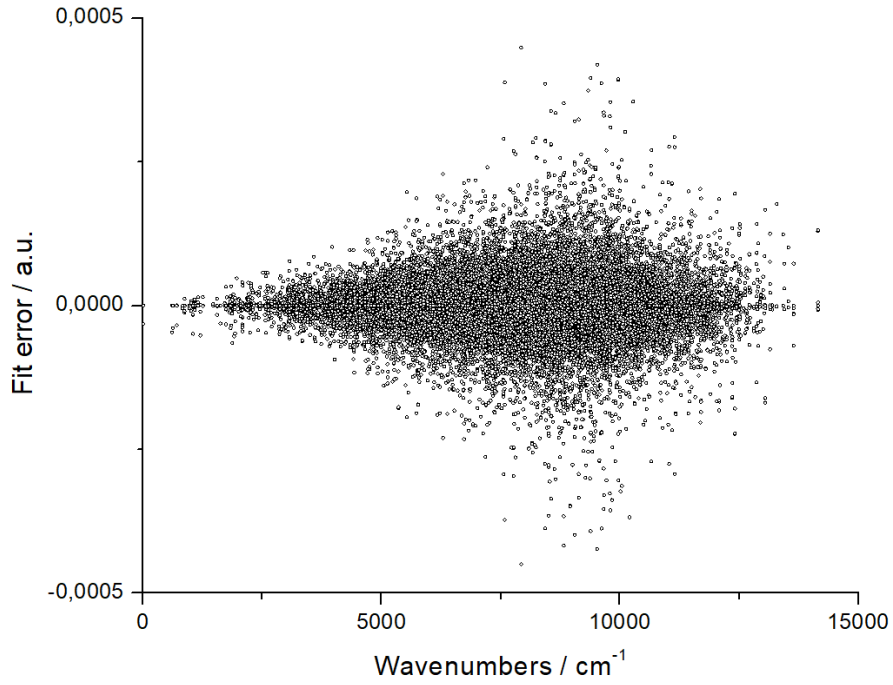

Fig. 2 *Fit error of the H_2CO analytical DMS to the ab initio values computed with the ACVQZ basis set.*

4. Ab initio effective Hamiltonian and dipole moment

To construct the effective Hamiltonian (H^{eff}), the PES reported in ref. [48] was used. The accuracy of the vibrational levels obtained from this PES is of the order of ~ 0.5 cm^{-1}. To improve the vibrational predictions, an empirical correction of the harmonic parameters of the PES was made.

The TENSOR code [82], [83], [84], [85] was then used to calculate the energy levels in normal coordinates using the Watson-Eckart kinetic energy operator. As an alternative to the contact transformation method described in Refs. [86], [87], the numerical approach proposed recently in [88] was used in the present work. It is based on the transformation of some variational eigenfunctions computed from the TENSOR code to derive an initial set of *ab initio* effective polyad Hamiltonian parameters to be refined on experimental data. Beyond obviating the need to make tedious algebraic calculations, the advantages of such an approach is threefold: (i) For a full account of symmetry, the irreducible tensor operator formalism is used at the very first stage of calculation, even for m belonging to non-Abelian point groups, (ii) In order to improve the accuracy of the effective parameters, variational energies can be replaced with empirical energy levels during the numerical block-diagonalization procedure (iii) Last but not least, a set of effective dipole moment parameters can be derived simultaneously from an *ab initio* DMS. Mathematically speaking, for a given polyad vector $\boldsymbol{c} = (c_1, c_2, c_3, \dots)^t$ such as the polyad number is $P = c_1\omega_1 + c_2\omega_2 + c_3\omega_3 + \cdots$, we search for a matrix transformation $\boldsymbol{T}^{(J,C)}$that brings $\boldsymbol{H}^{(J,C)}$into a block-diagonal form $\boldsymbol{H}^{(J,C,P)}$. Here, $\boldsymbol{H}^{(J,C)}$ is the matrix representation of the nuclear-motion Hamiltonian in a given basis set and for a given symmetry block (J, C). Following the iterative procedure in [88], effective Hamiltonian parameters are obtained by solving an overdetermined system of equations. The transformation $\boldsymbol{T}^{(J,C)}$ is then used to derive a set of effective dipole moment parameters in a similar fashion.

In this work, we start from the PES of ref. [48]. In order to better match observations, the equilibrium geometry as well as quadratic force constants were slightly empirically refined. The Eckart-Watson normal-mode Hamiltonian was expanded at order 18 and reduced at order 10 following the procedure described in [83]. The variational eigenpairs were computed up to $J = 5$ using the reduced 18→10 vibrational basis set. Using the polyad vector $\boldsymbol{c} = (2,1,1,1,2,1)^t$, an *ab initio* H^{eff} expanded at order 8 for the vibrational part and at order 6 for the vibration-rotation part was generated. This Hamiltonian is composed of 2740 tensor operators. As shown in ref. [88], the error on the energy levels calculated up to $J = 8$ between the variational calculation and the effective approach is of ~ 0.001 cm^{-1} around 5000 cm^{-1}. For line intensity predictions, the ab initio effective dipole moment operator for all transitions $P_i - P_j, i, j = 0,1,2,3$ was composed

of 1141 C_{2v} irreductible tensor operators. It was built from the DMS described in Section 3 following the method outlined in [88], and line intensity calculations were computed with the partition function of [89].

5. Spectra modeling and assignment: line parameters in the 3700–4450 cm^{-1} region

The origins of thirteen formaldehyde bands fall in the considered range, see **Fig. 1**. The transitions of the $v_3 + v_5$ band have been assigned in the work [59]. In the same work, the transitions of the $2v_2 + v_6$ band have been detected. Though the center of this band is above 4450 cm^{-1}, many weak lines of $2v_2 + v_6$ with large J fall into the considered spectral interval. The modeling of some bands from our range was made in the work [60], the correct centers of two bands $2v_3 + v_6$ and $v_3 + v_5$ were given in the same work, however without assignments of vibration-rotation lines. The work [67] provides a list of transitions with quantum identification. We made a comparison of the list of [67] by matching the same quantum numbers with the calculated transitions from our EH and EDM. In this comparison only 1303 transitions were taken with the consistent J, C identification for lower and upper levels and with a difference in wave numbers less than 0.005 cm^{-1}. This includes 1081 transitions of $v_3 + v_5$, 98 transitions of $v_4 + v_5$, 76 transitions of $v_1 + v_4$ and 33 transitions of $2v_2 + v_6$. Another 8 transitions of $3v_2$ and 7 of transitions of $2v_5$ from the list reported in ref. [67] were several orders of magnitude weaker than in our calculation, and we suspect than these assignments were wrong. The list of lines reported in recent ref. [67] in this range is clearly not complete: many strong observed transitions are absent there. The ExoMol linelist [45] was complete for $H_2{}^{12}C^{16}O$ transitions and agrees well with the main observed absorption features in the considered spectral range 3700-4450 cm^{-1} at low resolution. However, it did not have high-resolution accuracy for the line positions with some errors about 0.5 – 0.7 cm^{-1}.

As explained in the previous section, thirteen observed cold bands were analyzed in the present work using the H^{eff} constructed from the *ab initio* PES with a subsequent empirical optimization. First, few parameters specific to lower polyads were slightly adjusted to line positions. This generally led to calculated low-J line positions of thirteen bands to an uncertainty of about 0.1 cm^{-1}, except for some outliers. The program suite MIRS [90] was used to extend assignment to higher J iteratively assisted by the combinational difference method. More detail description of the assignment procedure and of the H^{eff} fit was already described in previous work devoted to spectra analyses of [91], [92], NF_3 [93], CF_4 [94] , methane [73],[74], [95], [96] and it isotopologues [97], [98]. Together with line intensities predicted from our *ab initio* DMS, this permitted to assign 6177 lines of H_2CO up to $J = 24$. The RMS (obs.-calc.) deviation for

these line positions in the range 3700-4450 cm^{-1} has quite rapidly converged to 0.001 cm^{-1} after a fine tuning of a subset of H^{eff} parameters. The band-by-band statistics of the line position fit using finally optimised effective Hamiltonian is shown in **Table 2.**

All positions and intensities were determined using the SpectraPlot software [99] from 4 experimental spectra specified in **Table 1**. The Voigt line shape profile with fixed self-broadening (see the next Section) and the instrumental function described in [100] were used in this work. Several examples of assigned spectra and absorption simulations using extracting line parameters from the observed spectra for various spectral intervals is shown in **Figs. 3-7**. Note, that the observed spectra in **Figs. 3-7** were recorded for low temperatures while the calculated linelist was converted to 296K. Although our analysis was limited to the indicated spectral interval covering thirteen bands in Table 2, the interaction H^{eff} parameters with upper vibrational states of the third polyad were also partly refined to account for the corresponding perturbations. Using a sample of measured intensities we have carried out a preliminary empirical optimization of few parameters of the effective dipole transition moments. This procedure will be finalized in the future work as soon as a complete analyses of the whole Polyad 3 are achieved.

Table 2. Line position statistics for assigned experimental transitions of H_2CO in the studied range

Vibrational upper state levels	Vibration Energy cm^{-1} This work	Line positions			
		Number of fitted lines	*RMS* $(10^{-3}\ cm^{-1})$	J_{min}	J_{max}
(000102) B_1	3676.611	47	1.48	3	17
(000003) B_2	3735.970	199	1.29	0	16
(001200) A_1	3826.05	7	3.04	3	10
(001101) A_2	3888.41	26	2.22	4	18
(001002) A_1	3935.491	101	0.85	3	18
(100100) B_1	3941.530	414	1.09	0	21
(000110) A_1	3996.519	302	1.20	1	19
(100001) B_1	4021.081	839	0.72	0	21
(010200) A_1	4058.358	361	1.01	0	20
(000011) A_1	4082.992	276	0.62	0	21
(010101) A_2	4164.720	384	0.74	1	18
(002100) B_1	4165.179	459	1.28	1	21
(002001) B_2	4192.383	718	0.67	0	23
(010002) A_1	4247.664	350	1.00	0	20
(101000) A_1	4255.457	69	1.31	3	16
(001010) B_2	4335.098	952	0.61	0	23
(011100) B_1	4397.745	227	1.04	4	21
(011001) B_2	4466.755	384	0.97	1	22
(003000) A_1	4495.	20	0.64	2	8
(110000) A_1	4529.	1	0.89	21	21
(010010) B_2	4571.	39	2.03	8	24
(020100) B_1	4624.	1	1.70	14	14
(012000) A_1	4729.	1	0.62	11	11
	Total	**6177**	**0.940**	**0**	**24**

The origins of the bands ν2+ ν3+ν6 and 3ν3 lie above our investigated spectral range, therefore ther determination using extrapolations of line series could be less accurate than for 18 other bands in Table 2. The ν3+ 2ν4, ν2+ ν4+ ν6 bands are very weak with few lines assigned in our spectra. For this reason , in both case we give approximate rounded values for the band origins.

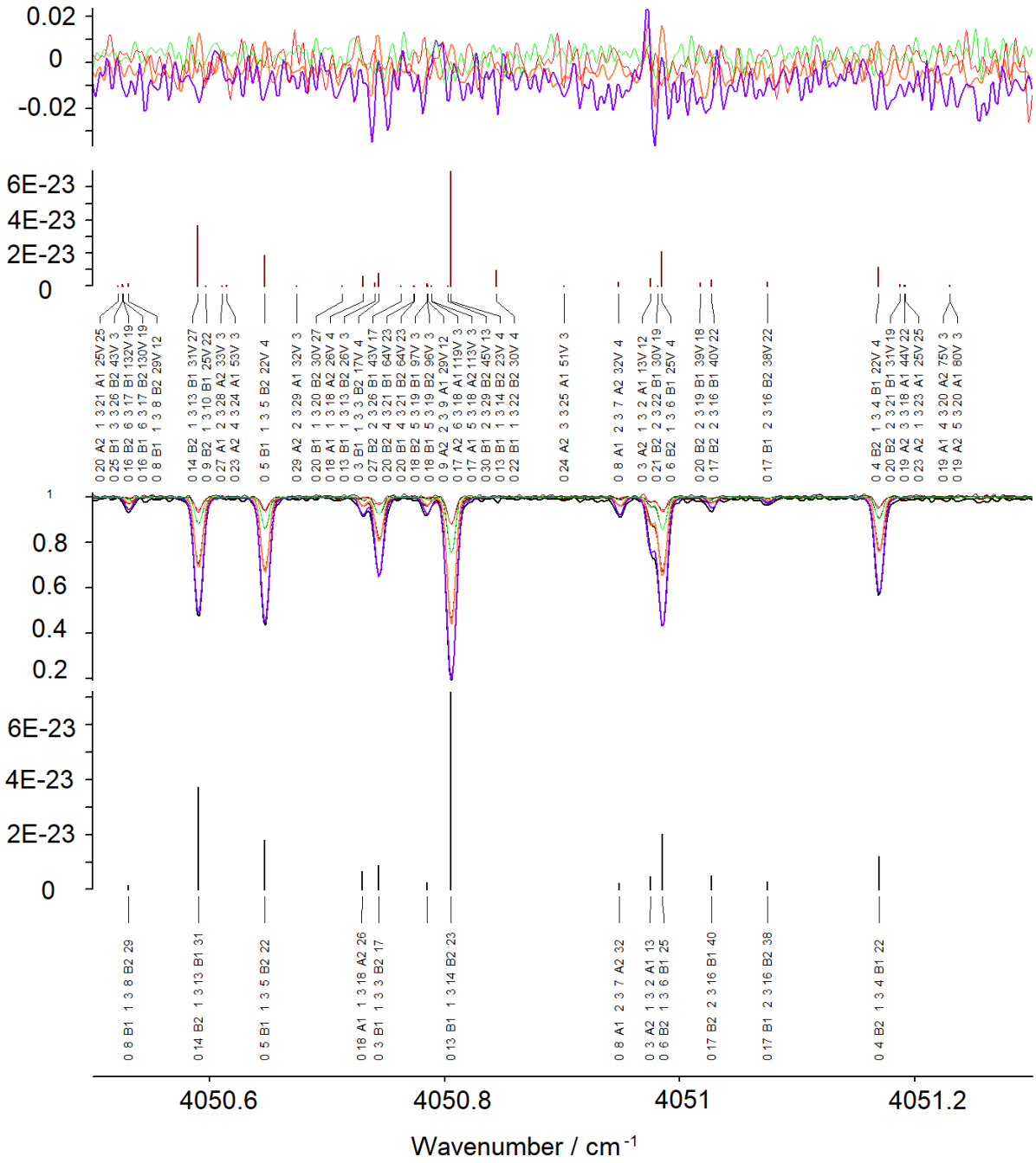

Fig. 3 *Example of quantum assignments in the $H_2{}^{12}CO$ spectra. The upper panel shows residuals (obs-calc) for three experimental spectra (green 0.053 Torr at 160 K, orange 0.165 Torr at 165 K and violet 0.315 Torr at 163 K). Next panel below shows our calculated line sticks at 296 K. The definition of the corresponding quantum numbers is given in Table 3. Next panel below shows three experimental spectra and three corresponded simulation spectra (green 0.053 Torr at 160 K, orange 0.165 Torr at 165 K and violet 0.315 Torr at 163 K). Next panel shows assigned experimental line list at 296 K.*

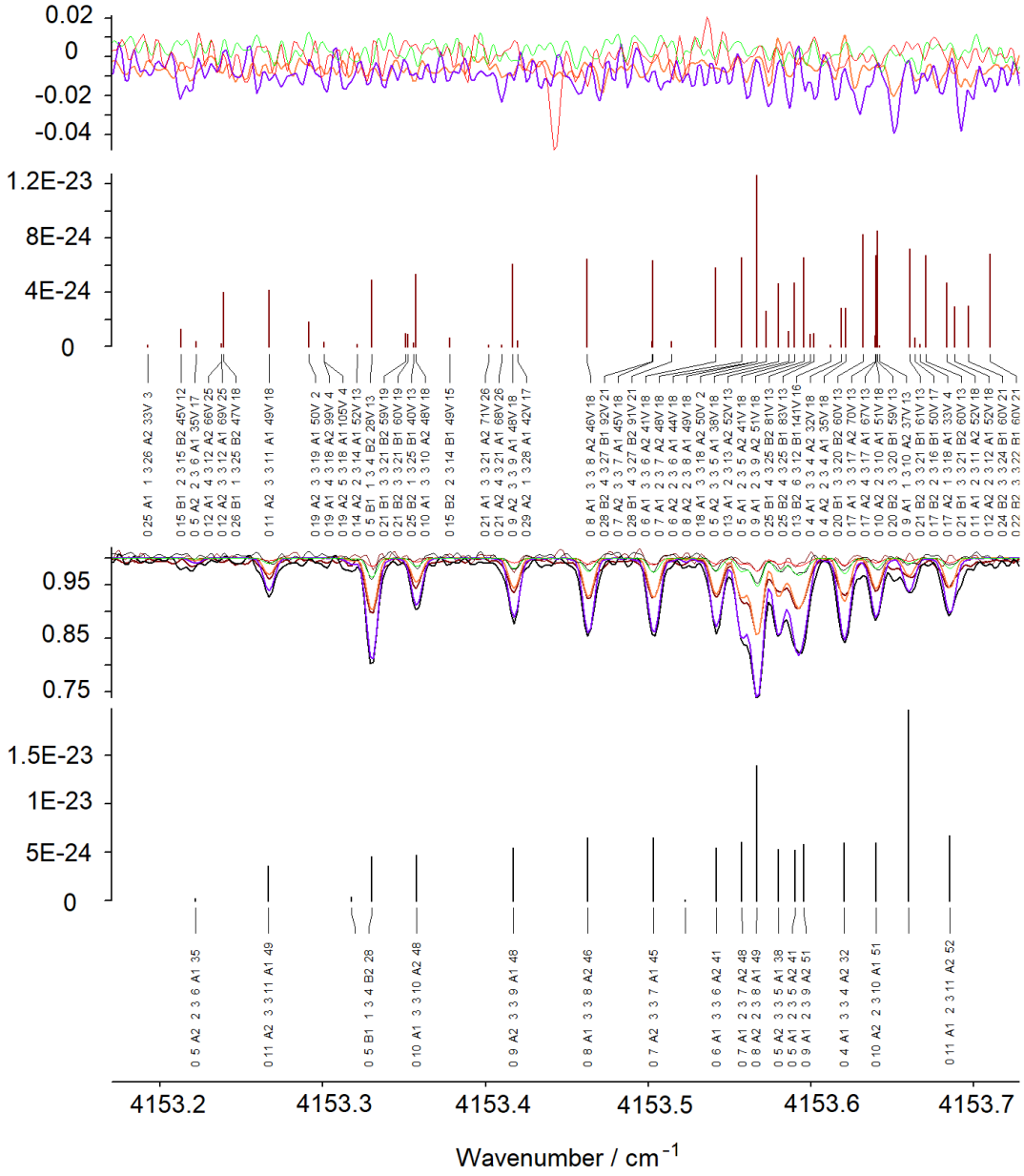

Fig. 4. *The same as in Fig. 3, except for the spectral range of 4153.2-4153.7 cm^{-1}*

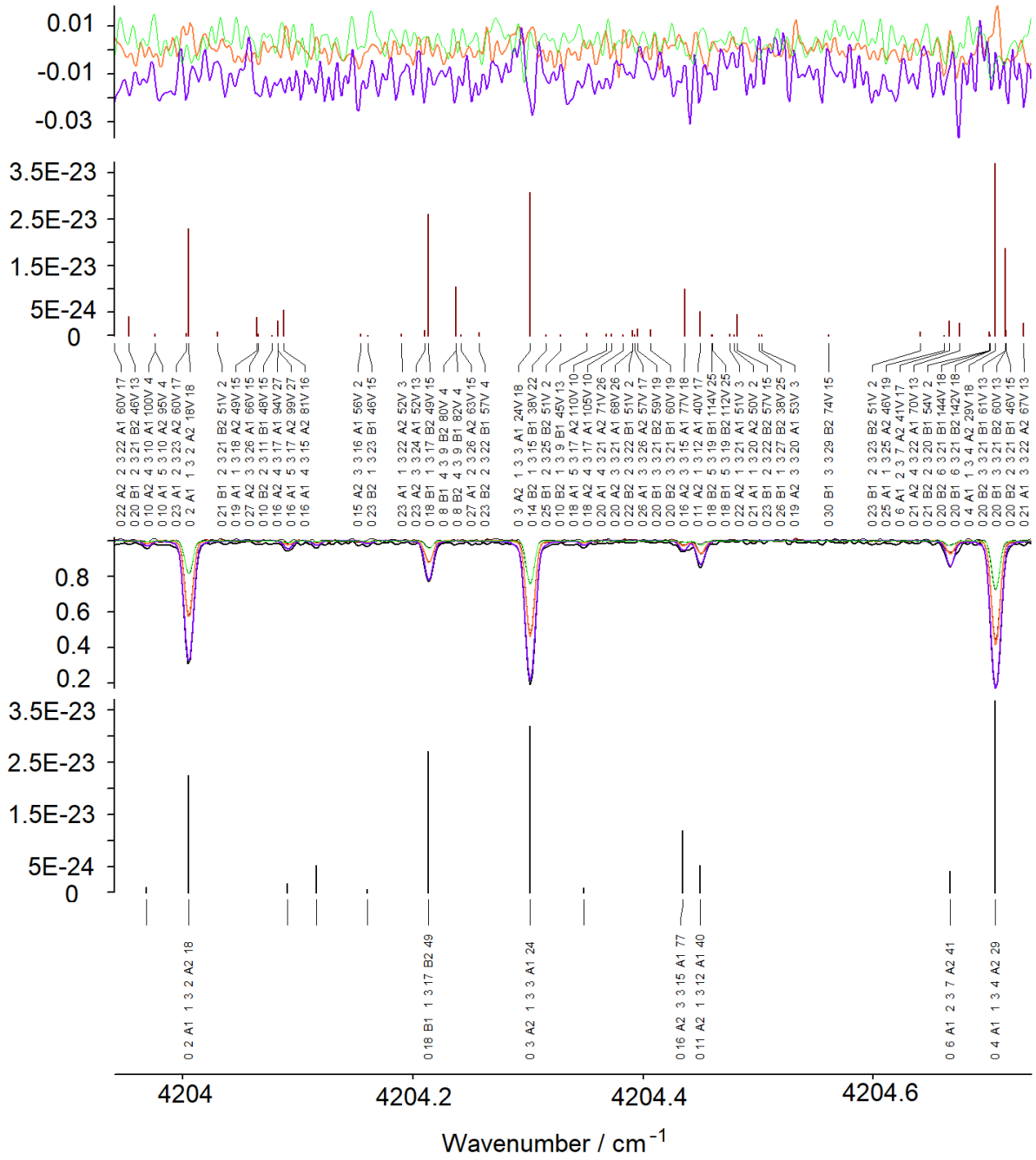

Fig. 5. *The same as in Fig. 3, except for the spectral range of 4204-4204.6 cm^{-1}*

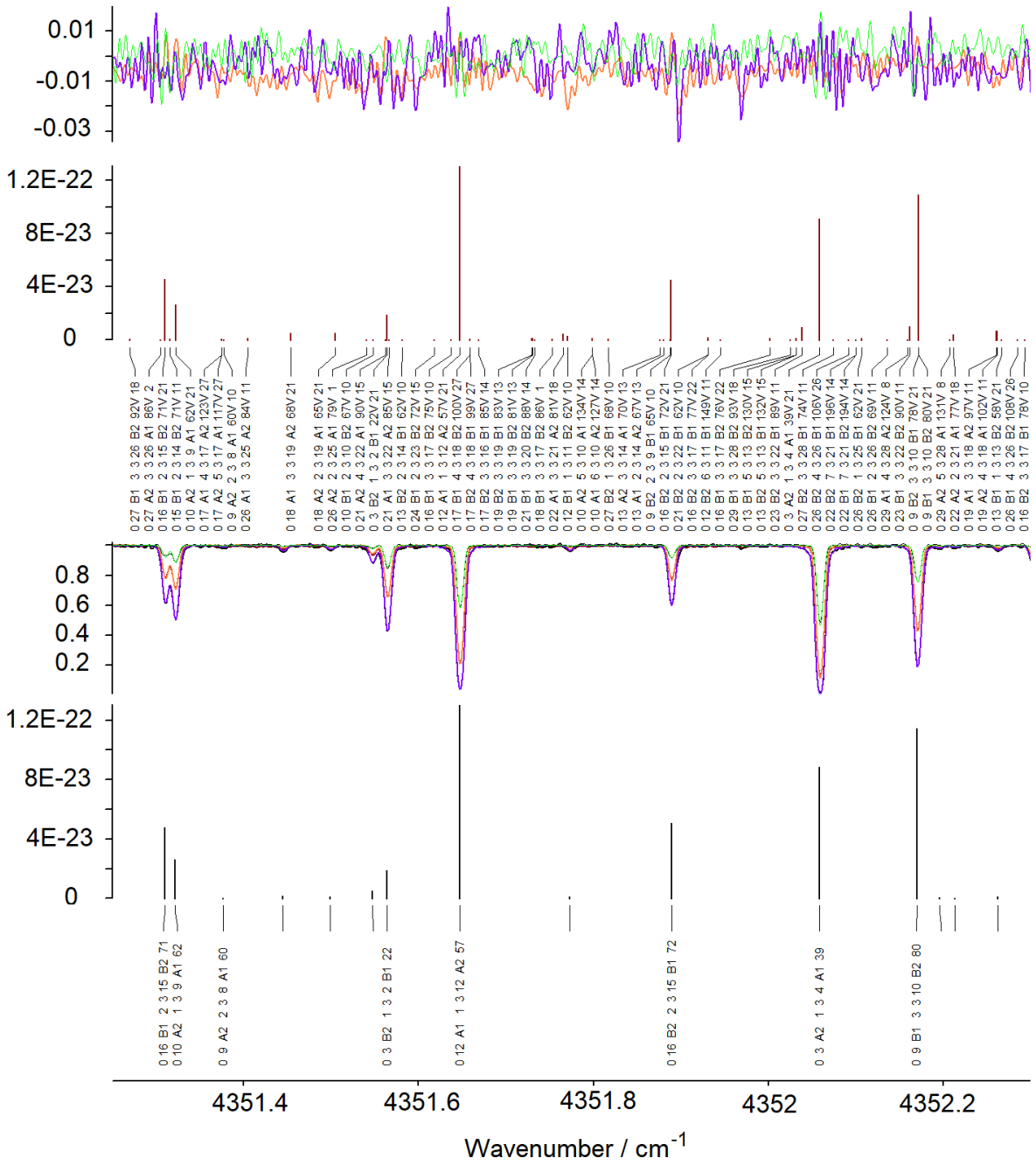

Fig. 6. *The same as in Fig. 3, except for the spectral range of 4351.4-4352.2 cm^{-1}*

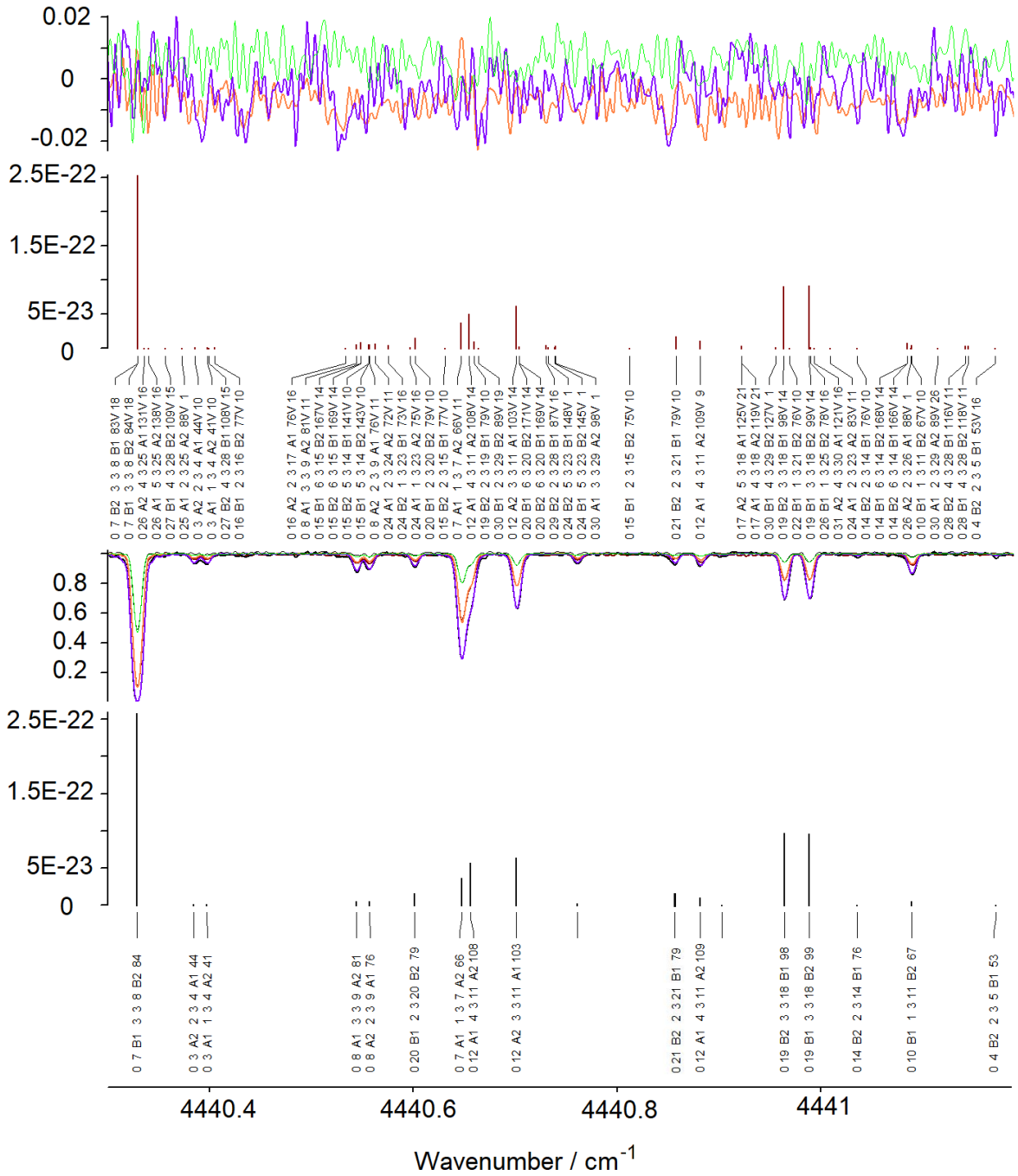

Fig. 7. *The same as in Fig. 3, except for the spectral range of 4440.4-4441 cm^{-1}*

6. Conclusion

Quantum assignments were made for 6177 transitions, which represent more 95% of the integrated line intensity at 160K and more 70% integrated line intensity at 296K in this region. Line positions were modeled with the empirically optimized effective Hamiltonian. Initial values of line intensities were computed from the ab initio dipole moment determined in this work transformed to the effective one following [88]. Using a sample of measured intensities we have

carried out a preliminary empirical optimization of few parameters of the effective dipole transition moments that led to the values included in the line list. The assigned line list which includes empirically fitted line positions and line intensities computed from our ab initio DMS is provided as a Supplementary Materials. The sample of the Supplementary material file is shown it **Table 3.**

Table 3. Sample of the line list of H_2CO at 296 K with assignment in the 3700-4450 cm^{-1} region provided as Supplementary Material.

Iso [a]	Key[b]	WvNm1[c] cm^{-1}	WvNm2[d] cm^{-1}	Intensity (296 K)[e] (cm/molecule)	Assignment (*P, J, C, N*)[f] Lower state	Upper state	*Upper Vibrational state*[g]	E_{low} (cm^{-1}) [k]
211	-	3700.6106	3700.6106	1.35e-24	0 12 B2 1	3 12 B1 8	000102 B1	190.843096
211	-	3700.6191	3700.6191	1.37e-24	0 2 B1 1	3 3 B2 5	000102 B1	15.720228
211	!	3700.8125	3700.8137	3.80e-25	0 8 A2 1	3 7 A1 9	000003 B2	120.129107
211	-	3700.9572	3700.9572	2.70e-25	0 17 A2 1	3 16 A1 7	000003 B2	363.872696
211	+	3701.0894	3701.0897	1.35e-24	0 2 B2 1	3 3 B1 4	000102 B1	15.236945
211	-	3701.1673	3701.1673	1.70e-25	0 26 B1 1	3 26 B2 8	000003 B2	871.974228
211	!	3701.1963	3701.1962	1.74e-24	0 14 B2 1	3 13 B1 8	000003 B2	253.823339
211	-	3701.2917	3701.2917	2.72e-25	0 14 A1 2	3 14 A2 7	000102 B1	290.956347
211	-	3701.5206	3701.5206	4.18e-25	0 12 B2 3	3 11 B1 16	000003 B2	393.771127
211	-	3701.5217	3701.5217	3.64e-25	0 12 B1 3	3 11 B2 16	000003 B2	393.771149
211	+	3701.6021	3701.6009	1.08e-24	0 7 B2 2	3 6 B1 9	000003 B2	141.713506
211	+	3701.6901	3701.6879	1.05e-24	0 7 B1 2	3 6 B2 9	000003 B2	141.708939
211	-	3701.9251	3701.9251	2.66e-25	0 9 A2 3	3 8 A1 13	000003 B2	240.203571
211	-	3701.9283	3701.9283	2.66e-25	0 9 A1 2	3 8 A2 12	000003 B2	240.203358

Notes:

[a] *always 211*

[b] *"+":assigned line, "-": unassigned line, "!": assigned upper level from other transition the upper energy level is assigned due to another transition*

[c] *measured line positions for assigned lines and calculated line positions for other.*

[d] *calculated line positions for all lines*

[e] *calculated line intensities at 296 K in cm/molecule.*

[f] *assignment for lower and upper state rovibrational assignments are given by the vibrational polyad number P, the rotational quantum number J, the rovibrational symmetry type C (C_{2v} irreducible representation) and the rovibration ranking index N.*

[g] *Upper vibrational state*

[k] *lower state energy (in cm^{-1})*

Absorption simulations in Figs 3-7 shows a good agreement with the observed cold spectra. In Figure 8 we give the comparison with available room-temperature low resolution PNNL spectra [101]. Theoretical simulations using our linelist in experimental conditions of PNNL (upper part) give a good agreement with PNNL cross section (lower part). Note that all half-widths were fixed at 0.018 cm^{-1}/atm, which may affect the heights of the observed peaks in the calculated spectra.

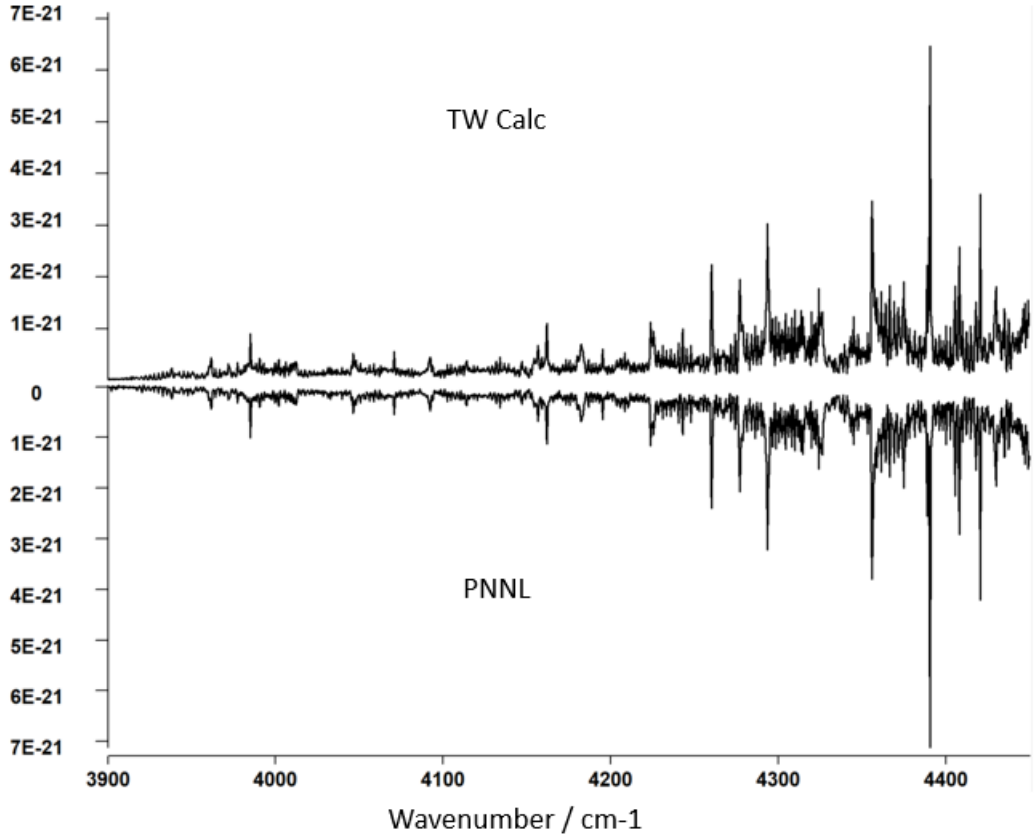

Fig 8. Comparison of the absorption cross-sections simulation at P=1000 mbar, T=296K, Halfwidth=0.018cm^{-1}/atm., using our line list (upper pane) with experimental room-temperature PNNL spectrum [101] (lower pane: upside down).

Comparison of simulation using our line list with the ExoMol lines list (updated by corrected line positions Marvell with empirical energy levels) at higher spectral resolution are plotted at the upper panels of Figure 9. Supplemental material file 2 contains 11 figures in 50 cm-1 scale (similar to figure 9) in the range 3700-4450 cm-1.

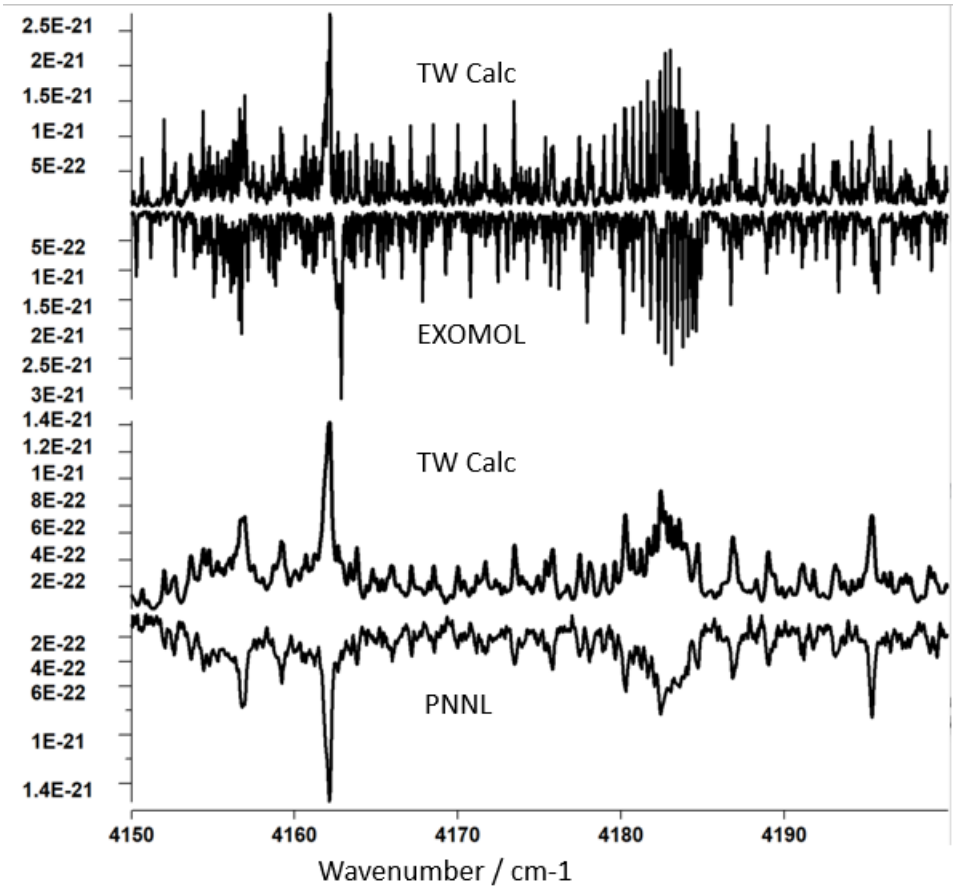

Fig 9. Upper panel: comparison of the absorption cross-sections simulation in the 4150-4200 cm-1 range at P=120 mbar using our line list with the simulation using updated ExoMol list at [69] (upside down). Lower panel: comparison of the absorption cross-sections simulation at P=1000 mbar using our line list experimental room-temperature PNNL spectrum [101] (upside down).

It is instructive to compare experimental band origins with the variational calculations using previously published PESs. Vibrational predictions in this range from ab initio PESs of the formaldehyde molecule have been reported in ref [42] and later in ref [48] The calculation accuracy in the latter work [48] was estimated to be no worse than 1 cm^{-1} that is confirmed by the comparison given in Table 4. High accuracy empirical band origins were calculated in refs. [60], [61], [62], [54] while low accuracy empirical band origins were given in ref. [66].

The empirical energy levels obtained with high accuracy coincided well with the calculated levels with the RMS deviation for thirteen band origins of 0.45 cm^{-1}. Note, that empirical levels obtained from low-resolution spectra [66] or from dark states analyses [60] were clearly less accurate.

Table 4. Comparison of $H_2{}^{12}CO$ band origins computed from published PESs [42]**,** [48] **with the empirical values determined in this work in the range 3470 - 4400 cm^{-1}**

Vib. State	C	Centre TW	Calc [51]	Exp-Calc [48]	Calc [42]	Exp-Calc [42]
$2v_2$	A_1	3471.715	3472.69	-0.975	3469.39	2.33
$3v_4$	B_1	3481.494	3480.76	0.734	3478.04	3.45
$2v_4 + v_6$	B_2	3587.022	3586.19	0.832	3581.09	5.93
$v_4 + 2v_6$	B_1	**3676.610**	3676.03	0.58	3668.88	7.73
$3v_6$	B_2	3735.970	3735.54	0.43	-	-
$v_3 + 2v_4$	A_1	3826.074	3825.74	0.334	3822.43	3.64
$v_3 + v_4 + v_6$	A_2	**3888.412**	3888.10	0.312	3883.37	5.04
$v_3 + 2v_6$	A_1	**3935.512**	3935.09	0.422	3929.86	5.65
$v_1 + v_4$	B_1	3941.530	3941.57	-0.04	3939.85	1.68
$v_4 + v_4$	A_2	3996.519	3995.94	0.579	3994.75	1.77
$v_1 + v_6$	B_2	4021.081	4021.18	-0.099	4017.7	3.38
$v_2 + 2v_4$	A_1	4058.357	4058.28	0.077	4054.6	3.76
$v_5 + v_6$	A_1	4082.992	4082.54	0.452	4078.88	4.11
$v_2 + v_4 + v_6$	A_2	**4164.719**	4164.74	-0.021	4159.35	5.37
$2v_3 + v_4$	B_1	4165.179	4165.37	-0.191	-	-
$2v_3 + v_6$	B_2	4192.383	4192.51	-0.127	4189.62	2.76
$v_2 + 2v_6$	A_1	4247.663	4247.79	-0.127	4241.02	6.64
$v_1 + v_3$	A_1	**4255.456**	4255.86	-0.404	4253.86	1.60
$v_3 + v_5$	B_2	4335.098	4335.05	0.048	4334.78	0.32
$v_2 + v_3 + v_4$	B_1	4397.747	4398.14	-0.393	4394.05	3.70
RMS deviation				**0.45**		**4.27**

Vibrational-rotational energy levels and linelists will be included in future edition of the TheoReTS database [102].

Acknowledgments

Support from the ANR-RNF TEMMEX project (grants ANR-21-30CE-0053-01 and RSF 22-42-09022) is acknowledged.

References

[1] Mangum J.G. , Wootten A., Formaldehyde as a probe of physical conditions in dense molecular clouds *Astrophys J. Suppl Ser* 1993;89: 123.

[2] Milam S.N., Remijan A.J., Womack M.,et al., Formaldehyde in comets C/1995 O1 (Hale-Bopp), C/2002 T7 (LINEAR), and C/2001 Q4 (NEAT): investigating the cometary origin of H2CO *Astrophys J* 2006;649: 1169.

[3] Sargent B.A., Forrest W., Watson D.M., D'Alessio P., Calvet N., Furlan E, al. et, Emission from water vapor and absorption from other gases at 5–7.5 ?m in Spitzer-IRS spectra of protoplanetary disks *Astrophys J.* 2014;792: 83.

[4] Nielsen G.D. , Wolkoff P., Cancer effects of formaldehyde: a proposal for an indoor air guideline value *Arch Toxicol* 2010;84: 423–446.

[5] Barbe A., Marche´ P., Secroun C., Jouve P., Measurements of tropospheric and stratospheric H2CO by an infrared high resolution technique. *J. Geophys. Res. Lett.* 1979;6: 463–465.

[6] Khare P., Kumar N., Kumari K.M., Srivastave S.S., Atmospheric formic and acetic acids: An overview. *Rev. Geophys.* 1999;37: 227.

[7] Kakabokas P., Carlier P., Fresnet P., Mouvierg G., Toupance G., Field studies of aldehyde chemistry in the Paris area. *Atmos. Environ.* 1988;22: 147-155.

[8] Zhu L., Abad G.G., Nowlan C.R., Miller C.C., Chance K, Ape E.C., DiGangi J.P., Fried A., Hanisco T.F., Hornbrook R.S., Hu L., Validation of satellite formaldehyde (HCHO) retrievals using observations from 12 aircraft campaigns *Atmos. Chem. Phys.* 2020;20: 12329–12345.

[9] Steck T., Glatthor N., Von Clarmann T., Fischer H., Flaud J.M., Funke B., Grabowski U., Höpfner M., Retrieval of global upper tropospheric and stratospheric formaldehyde (H2CO) distributions from high-resolution MIPAS-Envisat spectra *Atmos. Chem. Phys.* 2008;8: 463-470.

[10] Dufour G., Szopa S., Barkley M.P., Boone C.D., Perrin A., Palmer P.I., Bernath P.F., Global upper-tropospheric formaldehyde: Seasonal cycles observed by the ACE-FTS satellite instrument *Atmos. Chem. Phys.* 2009;9: 3893-3910.

[11] Partridge H. , Schwenke D.W., The determination of an accurate isotope dependent potential energy surface for water from extensive ab initio calculations and experimental data *J. Chem. Phys.* 1997;106: 4618-4639.

[12] Tyuterev V.G., Kochanov R.V., Tashkun S.A., Accurate ab initio dipole moment surfaces of ozone: First principle intensity predictions for rotationally resolved spectra in a large range of overtone and combination bands *J. Chem. Phys.* 2017;146: 064304.

[13] Yurchenko S.N., Mellor T.M., Freedman R.S., Tennyson J., ExoMol line lists – XXXIX. Ro-vibrational molecular line list for CO2 *Monthly Notices of the Royal Astronomical Society* 2020;496: 5282–5291.

[14] Huang X., Freedman R.S., Tashkun S., Schwenke D.W., Lee T.J., AI-3000K Infrared line list for hot CO2 *J. Molec. Spectrosc.* 2023;392: 111748.

[15] Polyansky O., Kyberis A., Zobov N., Tennyson J., Yurchenko S., Lodi L., ExoMol molecular line lists XXX: a complete high-accuracy line list for water *MNRAS* 2018;480, no. 2: 2597-2608.

[16] Huang X., Schwenke D.W., Lee T.J., Rovibrational spectra of ammonia. I. Unprecedented accuracy of a potential energy surface used with nonadiabatic corrections *J. Chem. Phys.* 2011;134, no. 4: 044320.

[17] Sousa-Silva C., Yurchenko S.N., Tennyson J., A computed room temperature line list for phosphine *J. Molec. Spectrosc.* 2013;288: 28-36.

[18] Nikitin A.V., Rey M., Tyuterev Vl.G, High order dipole moment surfaces of PH3 and ab initio intensity predictions in the Octad range *J. Molec. Spectrosc* 2014;305: 40-47.

[19] Rey M., Nikitin A.V., Tyuterev V.G., Accurate Theoretical Methane Line Lists in the Infrared up to 3000 K and Quasi-continuum Absorption/Emission Modeling for

Astrophysical Applications *Astrophys. J.* 2017;847: 105.

[20] Wong A, Bernath P.F., Rey M., Nikitin A.V., Tyuterev V.G., Atlas of Experimental and Theoretical High-temperature Methane Cross Sections from T=295 to 1000K in the Near-infrared *Astrophys. J. Supplement Series* 2019;240: 4.

[21] Rey M., Chizhmakova I.S., Nikitin A.V., Vl.G. Tyuterev, Understanding global infrared opacity and hot bands of greenhouse molecules with low vibrational modes from first-principles calculations: The case of CF4 *Phys. Chem.Chem. Phys.* 2018;20, no. 32: 21008-21033.

[22] Nikitin A.V., Rey M., Tyuterev Vl.G., First fully ab initio potential energy surface of methane with a spectroscopic accuracy *J. Chem. Phys.* 2016;145: 114309.

[23] Rey M, Nikitin A.V., Bézard B., Rannou P., Coustenis A., Tyuterev V.G., New accurate theoretical line lists of 12 CH 4 and 13 CH 4 in the 0–13400 cm−1 range: Application to the modeling of methane absorption in Titan's atmosphere *Icarus* 2018;303: 114-130.

[24] Yurchenko S.N., Barber R.J., Yachmenev A., Thiel W., Jensen P., Tennyson J., A Variationally Computed T = 300 K Line List for NH3 *J. Phys. Chem. A* 2009;113, no. 43: 11845–11855.

[25] Yurchenko S.N., Carvajal M., Thiel W, Jensen P., Ab initio dipole moment and theoretical rovibrational intensities in the electronic ground state of PH3 *J. Molec. Spectrosc.* 2006;239: 71-87.

[26] Owens A., Yurchenko S.N., Yachmenev A., Tennyson J., Thiel W., Accurate ab initio vibrational energies of methyl chloride *J. Chem. Phys.* 2015;142: 244306.

[27] Owens A., Yurchenko S.N., Yachmenev A., Thiel W., A global potential energy surface and dipole moment surface for silane *J. Chem. Phys.* 2015;143: 244317.

[28] Nikitin A.V., Rey M., Tyuterev V.G., Accurate line intensities of methane from first-principles calculations *Journal of Quantitative Spectroscopy and Radiative Transfer* 2017;200: 90-99.

[29] Yurchenko S.N., Owens A., Kefala K., Tennyson J., ExoMol line lists –LVII. High accuracy ro-vibrational line list for methane (CH4) *MNRAS* 2024;528: 3719–3729.

[30] Delahaye T., Nikitin A., Rey M., Szalay P., Tyuterev Vl.G., A new accurate ground-state potential energy surface of ethylene and predictions for rotational and vibrational energy levels *J. Chem. Phys.* 2014;141: 104301.

[31] Delahaye T., Nikitin A.V., Rey M., Szalay P.G., Tyuterev V.G., Accurate 12D dipole moment surfaces of ethylene *Chem. Phys. Letters* 2015;639: 275-282.

[32] Li J., Carter S., Bowman J.M., Dawes R., Xie D., Guo H., High-Level, First-Principles, Full-Dimensional Quantum Calculation of the Ro-vibrational Spectrum of the Simplest Criegee Intermediate (CH2OO) *J. Phys. Chem. Lett.* 2014;5, no. 13: 2364–2369.

[33] Mant B.P., Yachmenev A., Tennyson J., Yurchenko S.N., ExoMol molecular line lists – XXVII. Spectra of C2H4 *NMRAS* 2018;478: 3220–3232.

[34] Nikitin A.V., Rey M., Chizhmakova I.S., Tyuterev Vl.G., First Full-Dimensional Potential Energy and Dipole Moment Surfaces of SF6 *J. Phys. Chem. A* 2020;124, no. 35: 7014–7023.

[35] Rey M., Chizhmakova I.S., Nikitin A.V., Tyuterev V.G., Towards a complete elucidation of the ro-vibrational band structure in the SF6infrared spectrum from full quantum-mechanical calculations *PCCP* 2021;23: 12115-12126.

[36] Burleigh D.C., McCoy A.B., Sibert E.L. III, An accurate quartic force field for formaldehyde *J. Chem. Phys* 1996;104: 480.

[37] Martin, J. M. L.; Lee, T. J., An accurate ab initio Ouartic Force Field for Formaldehyde and its Isotopomers *J. Molec. Spectrosc.* 1993;160: 105-116.

[38] Burleigh D.C. , Sibert E.L., A random matrix approach to rotation-vibration mixing in H2CO and D2CO *J. Chem. Phys.* 1993;98: 8419-8431.

[39] Mladenovic M., Discrete variable approaches to tetratomic molecules Part II: application to H2O2 and H2CO *Spectrochimica Acta Part A* 2002;58: 809-824.

[40] Yagi K., Oyanagi C., Taketsugu T., Hirao K., Ab initio potential energy surface for vibrational state calculations of H2CO *J. Chem. Phys.* 2003;118: 1653-1660.

[41] Morgan W.J., Matthews D.A., Ringholm M., Agarwal J., Gong J.Z., Ruud K., Allen W.D., Stanton J.F., Schaefer H.F., Geometric Energy Derivatives at the Complete Basis Set Limit: Application to the Equilibrium Structure and Molecular Force Field of Formaldehyde *J. Chem. Theory Comput.* 2018;14: 1333−1350.

[42] Yachmenev A., Yurchenko S.N., Jensen P., Thiel W., A new “spectroscopic” potential energy surface for formaldehyde in its ground electronic state *J. Chem. Phys.* 2011;134: 244307-12.

[43] Poulin N.M., Bramley M.J., Carrington T., Kjaergaard H.G., Henry B.R., *J. Chem. Phys.* 1996;104: 7807.

[44] Carter S., Sharma A.R., Bowman J.M., Rosmus P., Tarroni R., Calculations of rovibrational energies and dipole transition intensities for polyatomic molecules using MULTIMODE *J. Chem. Phys.* 2009;131.

[45] Al-Refaie A. F., Yachmenev A., Tennyson J., Yurchenko S. N., "ExoMol line lists – VIII. A variationally computed line list for hot formaldehyde," *MNRAS*, vol. 448, pp. 1704-1714, 2015.

[46] Tennyson J. , Yurchenko S.N., The ExoMol project: Software for computing large molecular line lists *Int. J. of Quantum Chemistry* 2016;117: 92-103.

[47] Harding M.E., Metzroth T., Gauss J., Auer A.A., *J Chem. Theory Comput.* 2008;4: 64.

[48] Nikitin A.V., Protasevich A.E., Rodina A.A., Rey M., Tajti A., Tyuterev V.G., Vibrational levels of formaldehyde: Calculations from new high precision potential energy surfaces and comparison with experimental band origins *J. Quant. Spectrosc. Radiat. Transf.* 2021;260: 107478.

[49] Clouthier D.J. , Ramsay D.A., The spectroscopy of formaldehyde and thioformaldehyde. *Annu Rev Phys Chem* 1983;34: 31–58.

[50] Theule P, Callegari A, Rizzo T.R., Muenter J.S., Fluorescence detected microwave *J. Chem. Phys.* 2003;119: 8910–15.

[51] Luckhaus D, Coffey M.J., Fritz M.D., Crim F.F., Experimental and theoretical vibrational overtone spectra of vCH = 3, 4, 5, and 6 in formaldehyde (H2CO) *J.Chem Phys* 1996;104: 3472–8.

[52] Barry H, Corner L., Hancock G., Peverall R., Ritchie G., Cross sections in the 2v5 band of formaldehyde studied by cavity enhanced absorption spectroscopy near 1.76nm *Phys Chem Chem Phys 2002;4:445–50.* 2002;4: 445-50.

[53] Staak M, Gash E.W., Venables D.S., Ruth A.A., The rotationally-resolved absorption spectrum of formaldehyde from 6547 to 6804 cm-1 *J Mol. Spectrosc.* 2005;229: 115-21.

[54] Perez R., Brown J.M., Utkin Y., Han J., Curl R.F., Observation of hot bands in the infrared spectrum of H2CO *J. Molec. Spectrosc.* 2006;236: 151-157.

[55] Zhao W, Gao X, Deng L, Huang T, Wu T, Zhang W., Absorption spectroscopy of formaldehyde at 1.573 nm *J. Quant Spectrosc. Rad. Transf.* 2007;107: 331–9.

[56] Saha S, Barry H, Hancock G, Ritchie G.,Western, C.M., Rotational analysis of the 2v5 band of formaldehyde. *Mol Phys* 2007;105: 797–805.

[57] Tan T.L., Adawiah R., Ng L.L., The 2v2 bands of H212CO and H213CO by high-resolution FTIR spectroscopy *J Mol Spectrosc* 2017;340: 16–20.

[58] Jacquemart D, Laraia A, Tchana F.K., Gamache R.R., Perrin A, N. Lacome, Formaldehyde around 3.5 and 5.7 μm: measurement and calculation of broadening coefficients. *J Quant Spectrosc Rad Transf* 2010;111: 1209–22.

[59] Tipton T., Choe J.-I., Kukolich S.G., Fourier Transform Spectroscopy on the 3v2, 2v2 + v6 and v3 + v5 Bands of H2CO *J. Molec. Spectrosc. 114,239-256 (1985)* 1985;114: 239-256.

[60] Flaud J., Lafferty W., Sams R., Sharpe S., High resolution spectroscopy of H2 12C16O in the 1.9 to 2.56 μm spectral range *Molec. Phys.* 2006;104: 1891.

[61] Perrin A., Keller F., Flaud J.-M., New analysis of the v2, v3, v4, and v6 bands of formaldehyde H2 12C16O line positions and intensities in the 5–10 lm spectral region *J. Molec. Spectrosc.* 2003;221: 192-198.

[62] Perrin A., Valentin A., Daumont L., New analysis of the 2v4, v4+v6, 2v6, v3+v4, v3+v6, v1, v5, v2+v4, 2n3, v2+v6 and v2+v3 bands of formaldehyde H2 12C16O: Line positions and intensities in the 3.5 mm spectral region *J. molec. struct.* 2006;780–781: 28-44.

[63] KwabiaTchana F., Willaert F., Landsheere X, Flaud J-M, Lago L, Chapuis M, Herbeaux C., Roy P., Manceron L., A new, low temperature long-pass cell for mid-infrared to terahertz spectroscopy and synchrotron radiation use. *Rev. Sci. Instrum.* 2013;84: 093101.

[64] Ruth A.A., Heitmann U, Heinecke E., Fittschen C., The rotationally-resolved absorption spectrum of formaldehyde from 6547 to 7051 cm-1. *J Phys Chem* 2015;229: 1609–24.

[65] Fjodorow P, Hellmig O, Baev V.M., Levinsky H.B., Mokhov A.V., Intracavity absorption spectroscopy of formaldehyde from 6230 to 6420 cm−1 *Appl Phys B* 2017;123: 147.

[66] Bouwens R.J., Hammerschmidt J.A., Grzeskowiak M.M., Stegink T.A., Yorba P.M., Polik W.F., Pure vibrational spectroscopy of S 0 formaldehyde by dispersed fluorescence *J. Chem. Phys.* 1996;104: 460.

[67] Al-Derzi A.R., Tennyson J., Yurchenko S.N., Melosso M., Jiang N., Puzzarini C., Dore L., Furtenbacher T., Roland T., Csaszar A.G., An improved rovibrational linelist of formaldehyde, H2CO *J. Quant. Spectrosc. Radiat. Transf.* 2021;266: 107563.

[68] Furtenbacher T., Csaszar A.G., Tennyson J., MARVEL: measured active rotational–vibrational energy levels *J Mol Spectrosc* 2007;245: 115–25.

[69] (2024, June) www.exomol.com.

[70] Germann M., Hjalten A., Tennyson J., Yurchenko S.N., Gordon I.E., Pett C., Silander I., Krzempek K, Hudzikowski A., Gluszek A., Sobon G., Foltynowicz A., Optical frequency comb Fourier transform spectroscopy of formaldehyde in the 1250 to 1390 cm$^

[71] Daumont L., Nikitin A.V., Thomas X., Régalia L., Von der Heyden P., Tyuterev V., Rey M., Boudon V., Wenger C., Loëte M., Brown L.R., New assignments in the 2μm transparency window of the 12CH4 Octad band system. *J. Quant. Spectrosc. Radiat. Transfer* 2013;116: 101-109.

[72] Rey M., Nikitin A.V., Campargue A., Kassi S., Mondelain D., Tyuterev Vl.G., Ab initio variational predictions for understanding highly congested spectra: Rovibrational assignment of 108 new methane sub-bands in the icosad range (6280-7800 cm-1) *Phys. Chem.Chem. Phys.* 2016;16: 176-189.

[73] Nikitin A.V., Chizhmakova I.S., Rey M., Tashkun S.A., Kassi S., Mondelain D., Campargue A., Tyuterev Vl.G., Analysis of the absorption spectrum of 12CH4 in the region 5855-6250

cm-1 of the 2v3 band *J. Quant. Spectrosc. Radiat. Transfer.* 2017: https://doi.org/10.1016/j.jqsrt.2017.05.014.

[74] Rodina A.A., Nikitin A.V., Manceron L., Thomas X., Daumont L., Rey M., Sung K., Protasevich A.E., Tashkun S.A., Tyuterev V.G., Improved line list of 12CH4 in the 4100-4300 cm-1 region *J. Quant. Spectrosc. Radiat. Transfer.* 2022;279: 108021.

[75] Nikitin A.V., Protasevich A.E., Rey M., Serdyukov V.I., Sinitsa L.N., Lugovskoy A., Tyuterev Vl.G., Improved line list of 12 CH 4 in the 8850–9180 cm −1 region *J. Quant. Spectrosc. Radiat. Transfer* 2019;239: 106646.

[76] Foltynowicz A., Rutkowski L., Silander I., Johansson A., Silva de Oliveira V., Axner O., Soboń G., Martynkien T., Mergo P., Lehmann K., Measurement and assignment of double-resonance transitions to the 8900–9100-cm−1 levels of methane *PRL* 2021;103: 022810.

[77] Malarich N., Yun D., Sung K., Egbert S., Coburn S., Drouin B., Rieker G, Dual frequency comb absorption spectroscopy of CH4 up to 1000 Kelvin from 6770 to 7570 cm-1 *JQSRT* 2021;272: 107812.

[78] Nikitin A.V., Rey M., Campargue A., Tyuterev V.G., First assignments of the 6v4, v2+5v4, and v1+4v4 Triacontad band system of 12CH4 in the 7606-7919 cm-1 region *JQSRT* 2024.

[79] Dudas E, Vispoel B., Gamache R.R., Rey M, Tyuterev V.G., Nikitin A.V., Kassi S., Suas-David N., Georges R.*, Non-LTE spectroscopy of the tetradecad region of methane recorded in a hypersonic flow *Icarus* 2023;394: 115421.

[80] Gordon I.E., Rothman L.S., Hargreaves R.J., Hashemi R., Karlovets E.V., Skinner F.M., al et, The HITRAN2020 molecular spectroscopic database *J. Quant. Spectrosc. Radiat. Transfer.* 2022;277: 107949.

[81] Delahaye T., Armante R., Scott N.A., al. et, The 2020 edition of the GEISA spectroscopic database *Journal of Molecular Spectroscopy* 2021;380: 111510.

[82] Rey M., Group-theoretical formulation of an Eckart-frame kinetic energy operator in curvilinear coordinates for polyatomic molecules *J. Chem. Phys.* 2019;151: 024101.

[83] Rey M., Nikitin A.V., Tyuterev V.G., Complete nuclear motion Hamiltonian in the irreducible normal mode tensor operator formalism for the methane molecule *J. Chem. Phys* 2012;136, no. 24: 244106.

[84] Rey M., Nikitin A.V., Tyuterev Vl.G., First principles intensity calculations of the methane rovibrational spectra in the infrared up to 9300 cm-1. *Phys. Chem.Chem. Phys.* 2013;15, no. 25: 10049-10061.

[85] Rey M., Nikitin A.V., Tyuterev Vl.G., Convergence of normal mode variational calculations of methane spectra: Theoretical line list in the icosad range computed from potential energy and dipole moment surfaces *J. Quant. Spectrosc. Radiat. Transfer.* 2015;164: 207–220.

[86] Tyuterev VI.G., Tashkun S.A., Rey M., Kochanov R.V., Nikitin A.V., Delahaye T., Accurate spectroscopic models for methane polyads derived from a poten- tial energy surface using high-order contact transformations *J. Phys. Chem.* 2013;117: 13779–805.

[87] Tyuterev V.G., Tashkun S., Rey M, Nikitin A., High-order contact transformations of molecular Hamiltonians: general approach, fast computational algorithm and convergence of ro-vibrational polyad models *Molec. Phys.* 2022;120: e2096140.

[88] Rey M, Novel methodology for systematically constructing global effective models from ab initio-based surfaces: A new insight into high-resolution molecular spectra analysis *J.*

Chem. Phys 2022;292: 108349.

[89] Gamache R.R., Vispoel B., Rey M., Nikitin A., Tyuterev V., Egorov O., Gordon I.E., Boudon V., Total internal partition sums for the HITRAN2020 database *J. Quant. Spectrosc. Radiat. Transfer* 2021;271: 107713.

[90] Nikitin A.V., Rey M., Champion J.-P., Tyuterev Vl.G., Extension of the MIRS computer package for modeling of molecular spectra: from effective to full ab initio ro-vibrational hamiltonians in irreducible tensor form. *J. Quant. Spectrosc. Radiat. Transfer* 2012;113: 1034-1042.

[91] Nikitin A.V., Ivanova Y.A., Rey M., Tashkun S.A., Toon G.C., Sung, K., Tyuterev Vl.G., Analysis of PH3 spectra in the Octad range 2733–3660 cm-1 *J. Quant. Spectrosc. Radiat. Transf.* 2017;203: 472-479.

[92] Nikitin A.V., Campargue A., Protasevich A.E., Rey M., Sung K., Tyuterev Vl.G., Analysis of experimental spectra of phosphine in the Tetradecad range near 2.3 μm using ab initio calculations *Spectrochimica Acta Part A* 2023;302: 122896.

[93] Egorov O., Nikitin A.V., Rey M., Rodina A., Tashkun S., Tyuterev Vl.G., Global modeling of NF 3 line positions and intensities from far to mid-infrared up to 2200 cm −1 *J. Quant. Spectrosc. Radiat. Transf.* 2019;239: 106668.

[94] Mattoussi M., Rey M., Rotger M., Nikitin A.V., Chizhmakova I., Thomas X., Aroui H., Tashkun S., Tyuterev Vl.G., Preliminary analysis of the interacting pentad bands (v2 + 2 v4 , v2 + v3 , 4 v2 , v1 + 2 v2 , 2 v1) of CF 4 in the 1600 –1800 cm −1 region *J. Quant. Spectrosc. Radiat. Transfer* 2019;226: 92 - 99.

[95] Nikitin A.V., Thomas X., Daumont L., Rey M., Sung K., Toon G.C., Smith M.A.H., Mantz ProtasevichA.E., A.W., Tashkun S.A., Tyuterev Vl.G., Assignment and modelling of 12CH4 spectra in the 5550–5695, 5718–5725 and 5792–5814 cm−1 regions *J. Quant. Spectrosc. Radiat. Transfer* 2018;219: 323–332.

[96] Nikitin A.V., Thomas X., Regalia L., Daumont L., Rey M., Tashkun S.A., Tyuterev Vl.G., Brownc L.R., Measurements and modeling of long-path 12CH4 spectra in the 4800-5300 cm-1 region *J. Quant. Spectrosc. Radiat. Transfer* 2014;138: 116–123.

[97] Starikova E., Sung K, Nikitin A.V., Rey M., Mantz A, M.A.H Smith, The 13 CH 4 absorption spectrum at 80 K: Assignment and modeling of the lower part of the Tetradecad in the 4970–5470 cm −1 spectral range *J. Quant. Spectrosc. Radiat. Transfer.* 2018;206: 306-312.

[98] Nikitin A.V., Champion J.-P., Brown L.R., Preliminary analysis of CH3D from 3250 to 3700 cm−1. *J. Molec. Spectrosc.* 2006;240: 14-25.

[99] Nikitin A.V. , Kochanov R.V.Visualization and identification of spectra by the SpectraPlot, Visualization and identification of spectra by the SpectraPlot program. *Atmos Ocean Opt* 2011;24: 931-941.

[100] Dana V , Mandin J.-Y., NEW IMPROVEMENTS IN THE DETERMINATION OF LINE PARAMETERS FROM FTS DATA *J. Quant. Spectrosc. Radiat. Transfer* 1992;48: 725-731.

[101] Johnson T., Sams R., Sharpe S., The PNNL Quantitative Infrared Database for Gas-Phase Sensing: A spectral Library for Environmental, Hazmat, and Public Safety Standoff Detection. *Proceedings of SPIE - The International Society for Optical Engineering* 2004;5269: 159-169.

[102] Rey M., Nikitin A.V., Babikov Y., Tyuterev Vl.G., TheoReTS – An information system for theoretical spectra based on variational predictions from molecular potential energy and

dipole moment surfaces *J. Molec. Spectrosc.* 2016;327: 138–158.

397